
This is an electronic reprint of the original article.
This reprint may differ from the original in pagination and typographic detail.

Author(s): Jelovica, Jasmin & Romanoff, Jani & Ehlers, Sören & Aromaa, Jari
Title: Ultimate strength of corroded web-core sandwich beams
Year: 2013
Version: post print

Please cite the original version:

Jelovica, Jasmin & Romanoff, Jani & Ehlers, Sören & Aromaa, Jari. 2013. Ultimate strength of corroded web-core sandwich beams. *Marine Structures*. Volume 31. 1-14. DOI: 10.1016/j.marstruc.2012.12.001.

Rights: © 2013 Elsevier. This is the post print version of the following article: Jelovica, Jasmin & Romanoff, Jani & Ehlers, Sören & Aromaa, Jari. 2013. Ultimate strength of corroded web-core sandwich beams. *Marine Structures*. Volume 31. 1-14. DOI: 10.1016/j.marstruc.2012.12.001, which has been published in final form at <http://www.sciencedirect.com/science/article/pii/S0951833912000871>.

All material supplied via Aaltodoc is protected by copyright and other intellectual property rights, and duplication or sale of all or part of any of the repository collections is not permitted, except that material may be duplicated by you for your research use or educational purposes in electronic or print form. You must obtain permission for any other use. Electronic or print copies may not be offered, whether for sale or otherwise to anyone who is not an authorised user.

This is an author-generated copy of the publication:

Jelovica, J., Romanoff, J., Ehlers, S., Aromaa, J. Ultimate strength of corroded web-core sandwich beams. *Marine Structures* 31 (2013) p.1-14.

<http://www.sciencedirect.com/science/article/pii/S0951833912000871>

Present copy corresponds to the published version exactly in terms of content.

Ultimate strength of corroded web-core sandwich beams

J. Jelovica^{1*}, J. Romanoff¹, S. Ehlers², J. Aromaa³

¹ Department of Applied Mechanics / Marine Technology, Aalto University, P.O. Box 15300, 00076 Aalto, Finland

² Department of Marine Technology, Norwegian University of Science and Technology, 7491 Trondheim, Norway

³ Department of Materials Science and Engineering, Aalto University, P.O. Box 16200, 00076 Aalto, Finland

Keywords: web-core sandwich; ultimate strength; corrosion; three-point bending; stress-strain.

Abstract: The corrosive marine environment is a threat to the ultimate strength of steel sandwich structures. Therefore, ultimate strength experiments were carried out in three-point bending for beams with different corrosion exposure times, i.e. one and two years. Standard laser-welded web-core sandwich beams are studied and different corrosion protection systems considered. The beams experienced general corrosion. The thickness reduction in unprotected plates and laser welds is around the typical 0.1 mm/year. This led to an ultimate strength reduction of 10% and 17% for beams with exposure times of one and two years, respectively. The experimental ultimate strength is in agreement with finite element simulations. The ultimate strength was maintained for the beams protected with coating or closed-cell polyurethane (PU) foam.

1 Introduction

Steel sandwich panels bring a reduction in terms of weight and production cost in comparison to the traditional stiffened plates in marine structures [1, 2]. Web-core sandwich panels have been used there the most. The structure is made of orthogonal plates, which are periodic in the transverse direction and joined to the face-plates by laser welding; see Fig. 1. However, besides other factors, their broad application is limited by the concern that corrosion may affect the thin plates and thereby reduce the strength of the panels unfavourably. This is especially crucial if sea water enters the panel and all the steel surfaces are subject to corrosion.

Several authors have investigated the ultimate strength of web-core sandwich panels. Kolsters [3] and Romanoff [4] investigated the local ultimate strength of plate members of the sandwich panel under in-plane and out-of-plane loading. Kozak [5] studied the ultimate strength of steel sandwich columns under in-plane loading using experimental and numerical methods. The influence of corrosion on steel sandwich beams has been investigated in the EU Sandwich project [6] and DNV's investigation [7]. However, these experiments did not consider the ultimate strength. Hence, there is a need to investigate the influence of sea water exposure on the ultimate strength of sandwich structures.

The collapse of structural members is a function of geometrical and material strength properties. These properties change as a result of corrosion. Melchers et al. [8] showed that corroded plates have

* Corresponding author. Tel.: +358 9 4702 4172; fax.: +358 9 4702 4173.

E-mail address: jasmin.jelovica@aalto.fi

quite a complex surface profile. Boon et al. [9] and Almusallam et al. [10] observed that corrosion changes the stress-strain curve. They showed that the ductility becomes reduced and the material does not yield but starts strain-hardening from the onset of yielding. Ahmmad and Sumi [11] and Islam and Sumi [12] showed experimentally and numerically that the change in the stress-strain curve can be explained solely by the geometrical imperfections of the steel surface. These effects have to be accounted for in the ultimate strength study of a corroded structure.

This paper presents a series of ultimate strength tests on corroded web-core steel sandwich beams in three-point bending. The corrosion was achieved by submerging the specimens in the Baltic Sea for one and two years. Furthermore, different types of corrosion protection systems were used, including a core filling with polyurethane (PU) foam. Additionally, beams without corrosion were tested for comparison. In order to support the experimental investigation, finite element simulations were performed. In these, the plate thickness is considered constant and the material stress-strain curve is modified accordingly. As a result, the influence of corrosion on the sandwich beam ultimate strength is presented.

2 Experimental investigations

2.1 Beam specimens

Based on exposure time, three sets of sandwich beams are considered. Four unexposed specimens are tested as a reference. Two of these are untreated and two have foam in their core. The two other identical sets consisted of five specimens each, which were submerged in sea water for one and two years, respectively. These sets included beams with: no protection; paint outside and inside; paint outside and foam inside; paint outside and the inhibitor mixed with foam inside, and paint outside and the inhibitor applied to the steel surfaces before foam filling inside. The specimen nomenclature and a short description are presented in Table 1.

The nominal thickness of the face- and web-plates is 2.5 mm and 4.0 mm, respectively. The length of the beams is 1000 mm and the core height is 40 mm. The width of the beam is 300 mm. The cross-section of the beam is shown in Fig. 1. The closed-cell PU foam used was Edulan C-1746.2, with a density $\rho \approx 40 \text{ kg/m}^3$ and maximum elastic modulus $E_x \approx 8 \text{ MPa}$. Thus, the mechanical properties of the foam are low since the aim was only to prevent water from penetrating to the beam core. The surfaces were coated with Tikkurila Temacoat RM40 paint and/or protected with the Cortec VpCI-645 corrosion inhibitor mixed with the foam or Cortec VpCI-357 applied directly to the metal surfaces. For more details on the specimen preparation refer to Aromaa et al. [13]. The initial imperfections of the face-plates were measured prior to testing. The shape of the plates was found to be sinusoidal in both the longitudinal and transverse directions. The half-wave length was equal to the spacing of the web plates, 120 mm. The measured amplitude of imperfections was 0.4 mm (16% of the face-plate thickness).

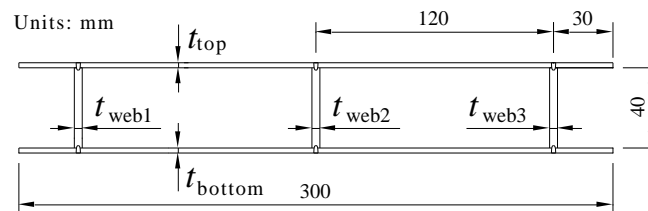


Fig. 1. The cross-section of the web-core sandwich beam.

2.2 Sea water corrosion tests

The exposed beams were submerged in the Baltic Sea for one and two years. They were placed two metres below sea level on a wooden rack positioned vertically to maximise the water flow around and inside the specimens as a result of wave motions. The test location was the Isosaari Marine Corrosion Station off Helsinki. The sea water is brackish water with a salinity of 4-6‰, which is highest in summer and lowest when the ice melts, a pH between 7.0-8.1, and a temperature variation from 0 °C in January to 15-16 °C from June to August.

2.3 Experimental set-up and test procedure

2.3.1 Ultimate strength experiments

The three-point bending test setup is shown in Fig. 2a. The experiments were displacement controlled. These were conducted in two phases. The first phase included two loading cycles of 0-8-0 kN to stabilise the force-deflection curves. In the second phase the deflection of the bottom face-plate was increased to 40 mm while the force was being measured. The ultimate strength was obtained during this process. The displacement sensor was located 16 mm away from the middle of the support span and 5 mm away from the central laser weld. An example of the beam under testing is shown in Fig 2b. Positioning the beam on the supports was performed with an accuracy of ± 1 mm in the x-direction. The position of the indenter relative to the top face plate was also ± 1 mm in the x-direction. More details on the test setup can be found in Jelovica et al. [14].

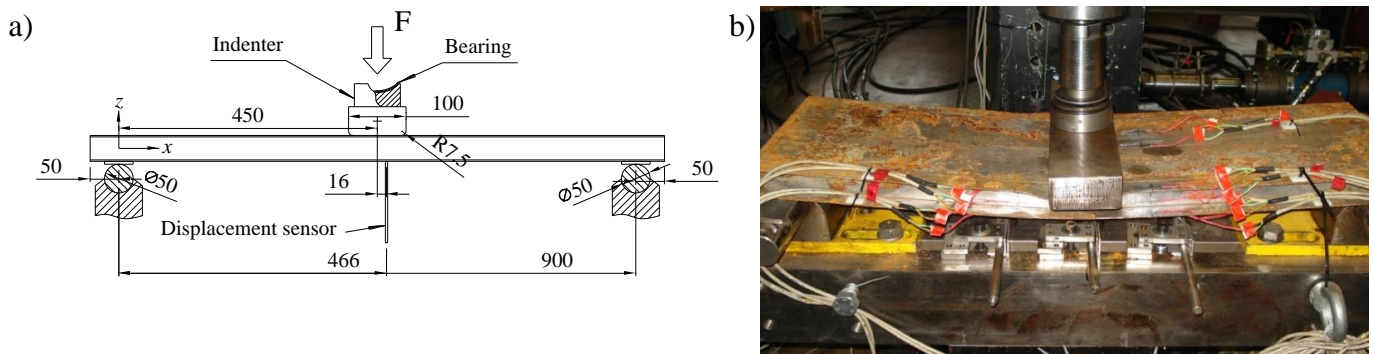


Fig. 2. a) Position of the beam and the indenter on the supports; b) Beam during testing.

2.3.2 Tensile tests and thickness measurements of the face- and web-plates

The stress-strain relationship for the face- and web-plates was determined with specimens cut out from the plastically undeformed parts of the beams, i.e. $x = 50$ mm to $x = 250$ mm and from $x = 650$ mm to $x = 850$ mm; see Fig. 3a. The specimens were produced according to DNV's specifications [15]; see Fig. 3b. The loading velocity in the tensile tests was 1.2 mm/min for all specimens. Altogether, 46 specimens were tested and the average was calculated separately for each plate and beam specimen. The tests were carried out with standard tensile testing equipment; see Jelovica et al. [14].

Thickness measurements were conducted on the tensile specimens before the testing. Rust was removed from the surfaces by using a steel wire brush on the specimens submerged in a 5% HCl solution. The original corroded surface was thus preserved. The thickness was measured with a digital micrometer at four and five locations in the width direction for the 2.5-mm- and 4.0-mm-thick specimens, respectively. This was repeated every 5 mm along the length of the gauge. The surface roughness of the

uncorroded specimens is inherently smoother and thus nine thickness measurements for the whole specimen were considered sufficient.

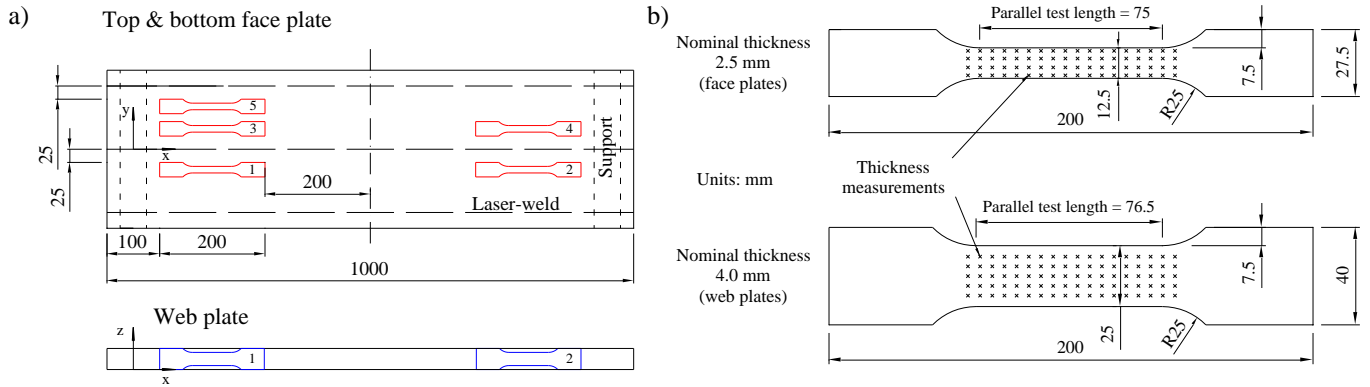


Fig. 3. a) Cut-out locations for the tensile specimens; b) Dimensions of the tensile specimens.

3 FE simulations

The behaviour of beams in three-point bending was simulated with the finite element solver LS-DYNA version 971. The simulations were performed for three untreated beams: uncorroded (0e1), one-year corroded (1e1) and two-year corroded (2e1). The aim was to support the experimental findings. The average stress-strain curves from the tensile tests were used for each face- and web-plate. The stress-strain curve for the laser-weld was obtained from Jutila [16]. The ultimate strength of the weld is 1100 MPa and the failure strain is 0.11. Material isotropy was assumed.

The shell element mesh is shown in Fig. 4a. A velocity of 50 mm/s was assigned to the indenter and the nodes at the junction between the top face-plate and the web-plate, below the corners of the indenter. There was an initial gap of 0.2 mm between the indenter and the face-plate. This was needed to allow the same physical deformations of the plates during the simulation as were observed in the experiments. Laser welds connect the nodes of the web and the face-plate; see Fig. 4a. Their thickness is 1.529 mm, which is the average of the measurements obtained by Romanoff et al. [17]. Harmonic imperfection field, imposed on the top face plate and assumed for all beam specimens, is presented in Fig. 4b. Details of the numerical modelling are presented in Appendix A.

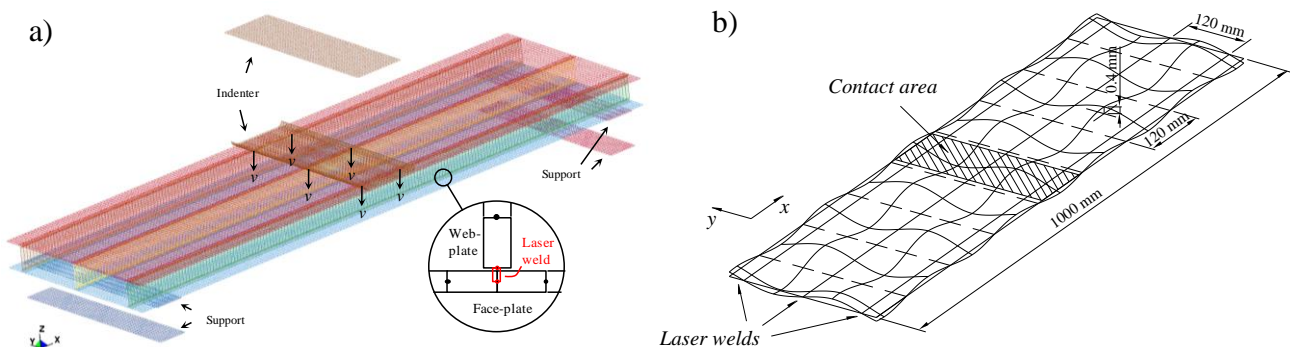


Fig. 4. a) FE mesh of the sandwich beam, indenter, and the supports; b) Imperfection field in all beam specimens.

4 Results

4.1 Geometrical and material properties of plates

The average measurements of plate thickness are presented in Table 1. These are graphically shown in Fig. 5a in addition to the other quartiles. No pattern of thickness change was observed along the specimen length. The thickness measurements are considered accurate since multiple measurements of the same point revealed a difference of up to 5 μm only. Fig. 5b presents the average thickness reduction per surface of the face-plates and inner and outer web-plates. The face-plates show the average corrosion rate of 0.08 mm per year. In outer web-plates, it decreases from 0.14 mm after the first year to 0.07 mm after the second year. The average corrosion rate is more stable for the inner web-plate, 0.11 mm and 0.10 mm after one and two years, respectively. The plates were mainly affected by general corrosion.

The average engineering stress-strain curves of the plates are presented in Fig. 6. Failure of the corroded specimens occurred by shear band formation. The average initial thickness over the width of the specimen, at the failure location, was used to determine the cross-sectional area for engineering stress calculation. The stress-strain curves were verified with finite element simulations of the tensile tests to obtain the corresponding force-elongation relationship. The same mesh size was used as for the sandwich beams. All the stress-strain curves, together with the averages, are presented in Appendix B.

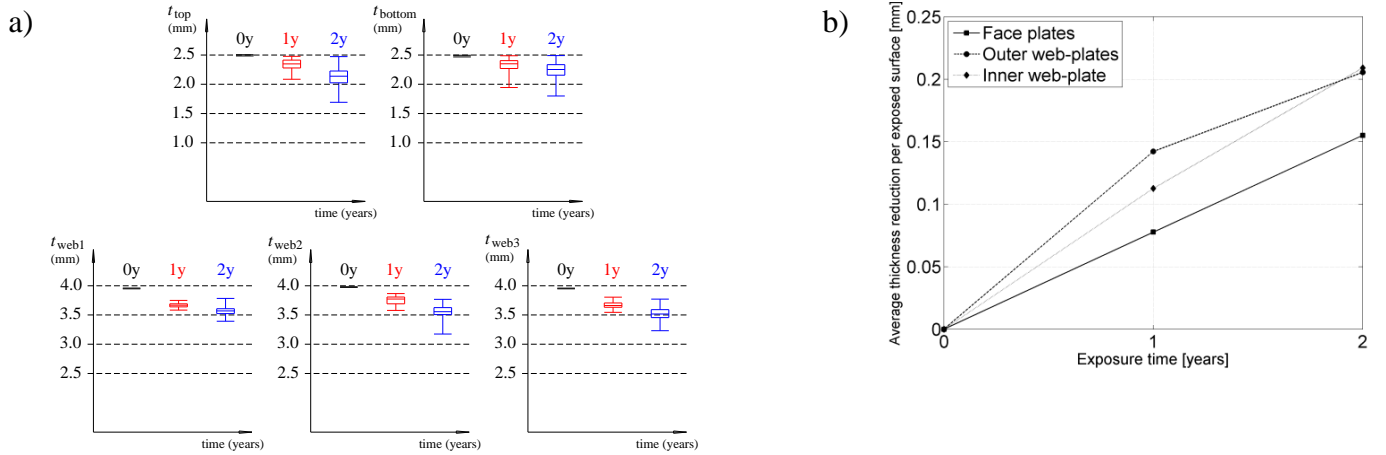


Fig. 5. a) Quartiles of the plate thickness measurements; b) Thickness reduction per surface of the unprotected beams.

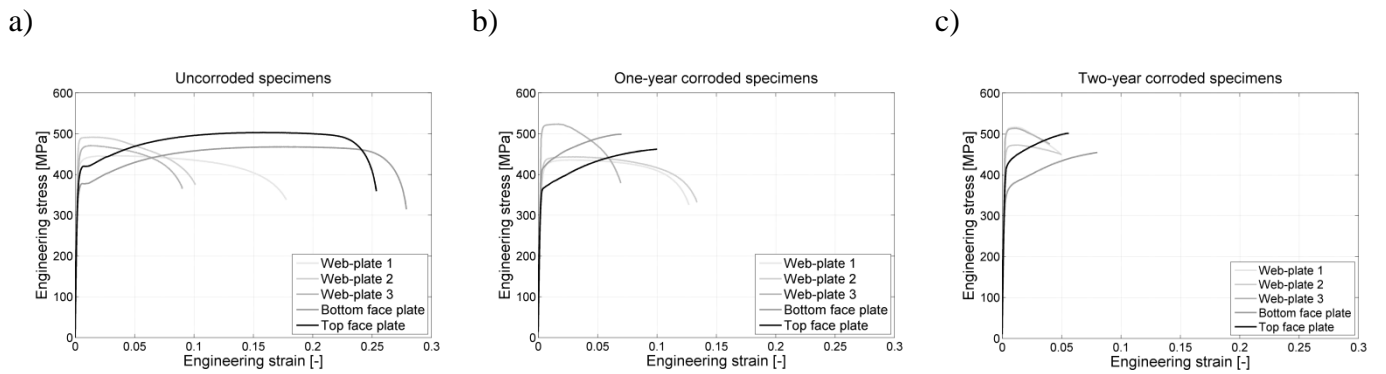


Fig. 6. Average engineering stress-strain curves for a) uncorroded; b) one-year corroded and c) two-year corroded beams.

4.2 Ultimate strength of beams

The force versus deflection of the untreated and the painted specimens is presented in Fig. 7. The ultimate strength of the uncorroded specimen 0e1 was 60.7 kN. The ultimate strength is defined as the maximum force that the beam carried. It decreased to 51.9 kN and 50.4 kN for the one- and two-year corroded specimens, respectively. Fig. 7 also shows finite element model simulations of the experiments. The simulated force-deflection curve of the uncorroded specimen with imperfections is in very good agreement with the experiment; see Fig. 7a. The ultimate strength is over-predicted by 0.9 kN (1.5%). The specimen with perfectly flat plates is shown for comparison. The ultimate strength of the one- and two-year corroded specimens was over-predicted by 2 kN (3.8%) and 2.5 kN (4.9%), respectively, when the average thickness measurements for the plates were used; see Fig. 7b and Fig. 7c. When the thickness was reduced by two standard deviations, the simulations under-predicted the ultimate strength by 2.5 kN (4.8%) and 4.7 kN (9.3%) in the same respect. Fig. 7d shows that painted beam specimens did not experience strength reduction.

The difference in yield strength between top and bottom face-plates is 40 MPa; see Fig. 6. In the uncorroded and two-year corroded specimens the top plate had a higher yield strength. Accidentally, the one-year corroded specimen was tested upside down, but the simulations show that an additional 2.7 kN are gained by turning the specimen; see Fig. 7b. This means that the ultimate strength of the one-year specimen would have been about 54.6 kN if it had been tested in the same way as the other two specimens.

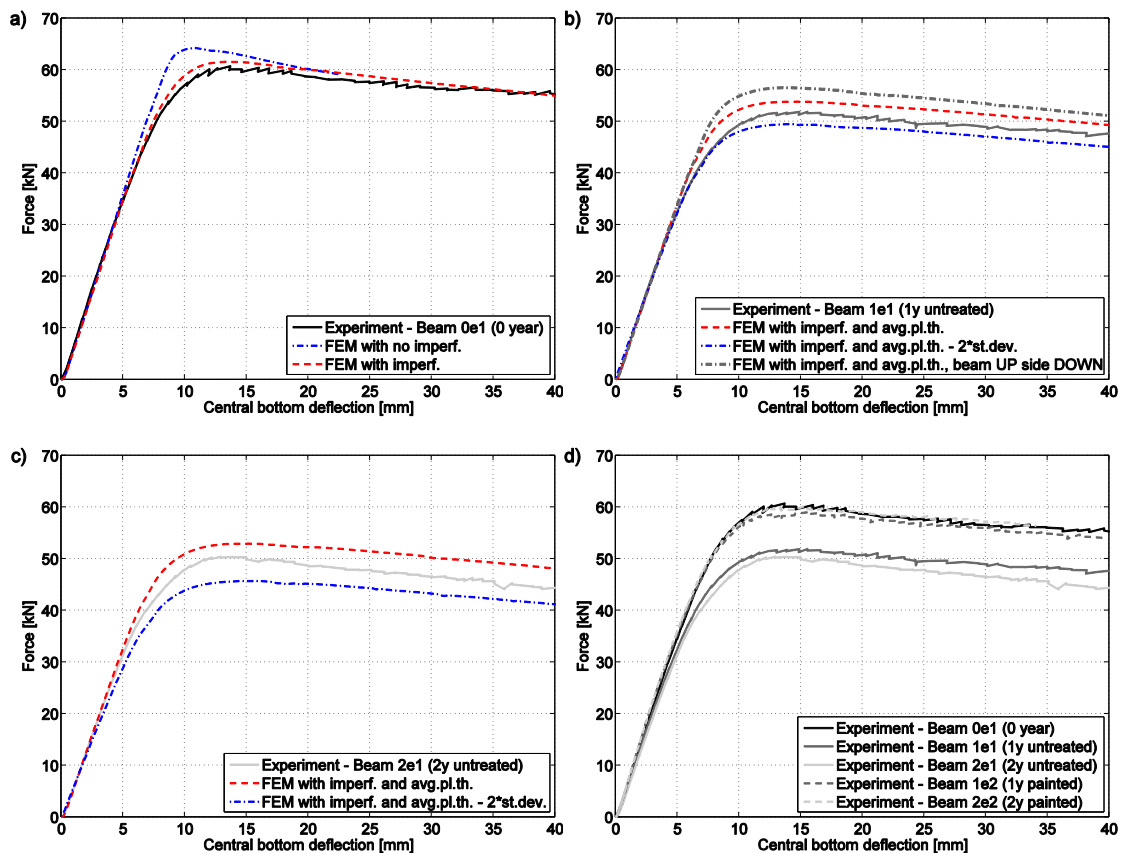


Fig. 7. Experimental and simulated force-deflection curves for the a) uncorroded (0e1); b) one-year corroded (1e1), and c) two-year corroded (2e1) beam. d) Experimental curves for untreated and painted beams with different exposure time.

	Name	Exterior condition	Interior condition	Ultimate strength [kN]	Plate thickness [mm]														
					Face-plate						Web-plate								
					Top			Bottom			1			2			3		
					Nom.	μ	σ	Nom.	μ	σ	Nom.	μ	σ	Nom.	μ	σ	Nom.	μ	σ
No corrosion	0e1	Untreated	Untreated	60.7	2.5	2.494	0.005	2.480	0.008	4.0	3.954	0.003	3.975	0.004	4.0	3.951	0.003		
	0e2	Untreated	Untreated	60.1															
	0f1	Untreated	Foam	63.1															
	0f2	Untreated	Foam	62.9															
One-year corrosion	1e1	Untreated	Untreated	51.9/54.6*		2.337	0.090	2.327	0.103		3.665	0.036	3.750	0.074		3.670	0.055		
	1e2	Paint	Paint	59.0		2.494	0.005	2.480	0.008		3.954	0.003	3.975	0.004		3.951	0.003		
	1f1	Paint	Foam	60.8															
	1f2	Paint	Inhibitor mixed with foam	61.4															
	1f3	Paint	Inhibitor on surfaces only and filled with foam	59.4															
Two-year corrosion	2e1	Untreated	Untreated	50.4		2.120	0.146	2.232	0.140		3.566	0.080	3.557	0.101		3.516	0.104		
	2e2	Paint	Paint	59.6		2.494	0.005	2.480	0.008		3.954	0.003	3.975	0.004		3.951	0.003		
	2f1	Paint	Foam	60.0															
	2f2	Paint	Inhibitor mixed with foam	60.0															
	2f3	Paint	Inhibitor on surfaces only and filled with foam	59.4															

Table 1. The nomenclature, ultimate strength, and plate thickness of the beams.

The ultimate strength of the specimens is presented in Table 1. The difference between the two uncorroded beams is 0.6 kN. The uncorroded specimen had an increase of about 4% in its ultimate strength when filled with foam. The protection of the specimens with foam was equally effective in preventing the strength reduction for the studied exposure time. However, Fig. 8b and Fig. 8c show foam degradation in two-year specimens that have the corrosion inhibitor mixed with foam or applied to the inner steel surfaces, respectively. On the other hand, the foam in the specimens with no inhibitor has good adhesion to steel surfaces and no voids; see Fig. 8a.

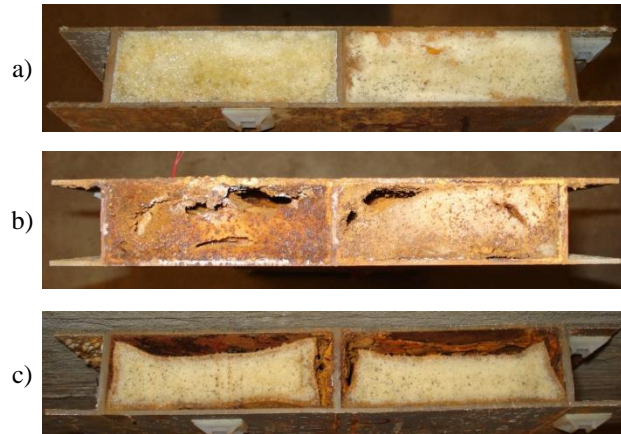


Fig. 8. Beam cross-section at $x = 50$ mm for two-year corroded beams protected with paint from outside and inside with a) foam applied to clean steel surfaces (2f1); b) foam mixed with inhibitor (2f2); c) foam applied to surfaces protected with inhibitor (2f3).

4.2.1 Sensitivity to the laser weld thickness

The state of the laser welds from the beams in this study was reported in Aromaa et al. [13]. The most significant thickness reduction was 30% for the specimen from the two-year corroded beam (2e1); see Fig. 9a. The initial thickness is estimated by the boundary of the heat-affected zone. The sensitivity of the ultimate strength to the thickness of the laser weld is presented in Fig. 9b. The results are obtained by reducing the weld thickness in FEA. It can be seen that the reduction of 30% of all the welds in the specimen resulted in an ultimate strength reduction of 1.4 kN (2.6%). The maximum strain in the laser weld at the end of the simulation was 0.1, thus the welds have not failed.

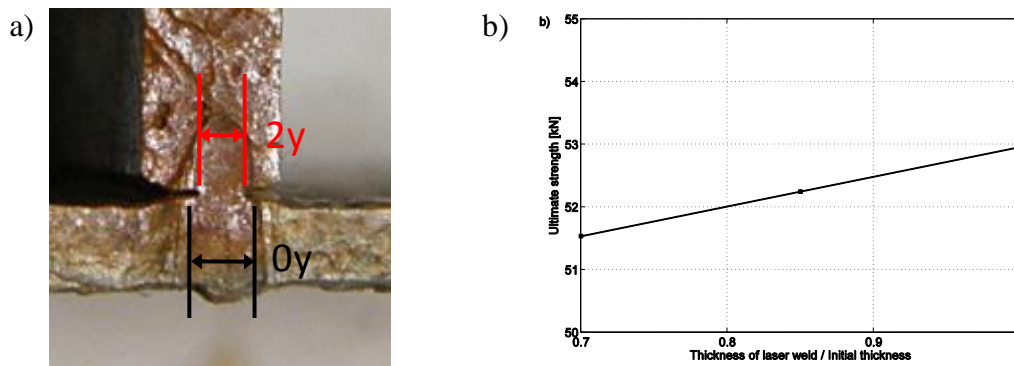


Fig. 9. a) Laser weld thickness in unprotected beam with two-year exposure time (2e1) – the worst observed reduction (Aromaa et al. [13]). Initial thickness is estimated by the boundary of the heat-affected zone; b) Ultimate strength sensitivity to laser weld thickness.

5 Discussion

The corrosion rate of the plate surfaces from the unprotected beams was 0.1 mm on average after the first year. This is a typical value reported in the literature for immersed plates; see e.g. Melchers [8]. The corrosion rate decreased for the second year, to 0.08 mm on average. The decrease can be explained by the formation of a protective corrosion product layer on the steel surfaces. The decrease of the corrosion rate is anticipated in prominent time-variant corrosion wastage model; see Guedes Soares and Garbatov [18]. The corrosion rate meant a 5.5% reduction in the face-plate thickness per year for the beam dimensions selected in this study.

Surface roughness becomes significant in a short period of time. After one year of corrosion, the standard deviation of the thickness distribution is equal to the average corrosion rate. After the second year, it is about 50% higher. Significant surface roughness was shown by Ahmmad and Sumi [11] to cause different stress-strain behaviour. Their study involved tests of tensile specimens with artificial pits in uncorroded steel and numerical simulations with solid elements. The same change in the stress-strain curve was observed here: ductility (failure strain) was reduced and the strain hardening commenced from the onset of yielding. Furthermore, as suggested in [11], the yield and ultimate strength of corroded material remain unchanged if they are calculated based on minimum sectional area of the specimen.

The ultimate strength reduction in three-point bending for the studied beam dimensions was 10% and 17% for beams with exposure times of one and two years. This is a rapid decrease in strength, considering that the structure should be in use for many more years. Nonetheless, this was the worst-case scenario. The beam had no protection from corrosion and was exposed to a water flow not only outside but also inside the sandwich beam. With a proper protection from corrosion, such a situation can be avoided, as presented in this investigation. Even for structural elements directly exposed to water flow, it has been shown that the breakdown of the coating, the most common type of corrosion protection system, takes between 2 and 10 years; see Guo et al. [19]. The experiments showed that the efficient protection of ultimate strength can be achieved by several corrosion protection systems. However, the corrosion inhibitor in combination with foam inside the beam core resulted in foam degradation.

Finite element simulations of ultimate strength experiments gave a 1.5% difference compared with the experimental force-deflection curve for the uncorroded beam. The difference increased to 5% for corroded beams when the average plate thickness and stress-strain curve were used; simulations over-predicted the ultimate strength. When the average plate thickness was decreased by two standard deviations (95% confidence interval), the simulations under-predicted the ultimate strength by 9%. Ahmmad and Sumi [11] used several solid elements through the plate thickness to accurately simulate the stress-strain behaviour of a tensile specimen with artificial pits. Such an approach would have been extremely inefficient for the sandwich beam, as presented by Romanoff et al. [20]. Nonetheless, the importance of accurate thickness to the ultimate strength is outlined in this study.

In addition to the plates, corrosion also affected the laser welds, where the reduction of the thickness was 30%. This had an effect of 2.6% on the ultimate strength, which is significantly less than presented by Romanoff et al. [20]. The reason for this discrepancy is the difference in the load and boundary conditions. However, if the corrosion progressed at the speed observed in this investigation, more significant strength problems might occur. Therefore, additional experiments are needed with longer exposure times.

6 Conclusions

This paper described ultimate strength experiments on web-core sandwich beams in three-point bending. The beams were divided into three groups on the basis of the corrosion extent: (i) uncorroded, and corroded for a duration of (ii) one and (iii) two years. The experimental ultimate strength is in agreement with FE simulations. The following conclusions are outlined:

- steel sandwich beams are prone to fast strength reduction if the protection against corrosion is ineffective and there is water inside and outside the beam;
- the surfaces of a steel sandwich beam can be successfully protected from corrosion with coating and closed-cell PU foam;
- the use of inhibitor inside the core results in foam degradation and exposes the inner surfaces to sea water within two years under the roughest conditions;
- in longitudinal three-point bending, the sandwich beam is not sensitive to laser weld corrosion wastage;
- FEA shows the importance of considering accurate plate thickness to the ultimate strength of corroded steel sandwich beams.

Appendix A – Details of the FE simulations

The simulations were carried out using the explicit time integration solver since the problem involves contact and large deformation of elements in the post-ultimate region of the response. It is a more robust choice than the implicit solver, which may not converge with increasing non-linearities; see Harewood and McHugh [21]. The structure was modelled using Belytschko-Lin-Tsay shell elements with five integration points through the thickness. This is the default shell element type in LS-DYNA. The stress-strain curves were implemented through material type 24. The curves were converted into true stress-strain values using ordinary logarithmic mapping. Standard LS-DYNA hourglass and time step control was used.

The finite element mesh is shown in Fig. 4. A support cylinder is represented as a pair of rigid flat rectangular meshes whose centre of rotation corresponds to that in experiments. The only degree of freedom allowed is rotation around the y-axis. The indenter is also treated as a rigid part. The lower of the two indenter meshes has rounded corners, which are important for contact when large deformations occur. All the rotational degrees of freedom are allowed, together with vertical translation. The contact is treated through the *CONTACT_AUTOMATIC_SINGLE_SURFACE scheme with an assumed static friction coefficient of 0.3; see Richardson and Nolle [22]. The reaction forces between the beam and the indenter are obtained via the *CONTACT_FORCE_TRANSDUCER_PENALTY command.

The mesh size was the following: 20 elements for the face-plate between the neighbouring web-plates and 12 elements per height of the web-plate. The element length next to the weld was reduced by half. This is sufficient to accurately predict the deformed shape of the plates and thus the ultimate strength of the beam. Refinement of the mesh size by 50% resulted in only a 1% change in the ultimate strength and was therefore not used.

Appendix B – Stress-strain curves

The stress-strain relationship of the tested tensile specimens is presented in Fig. B.1a – Fig. B.3b.

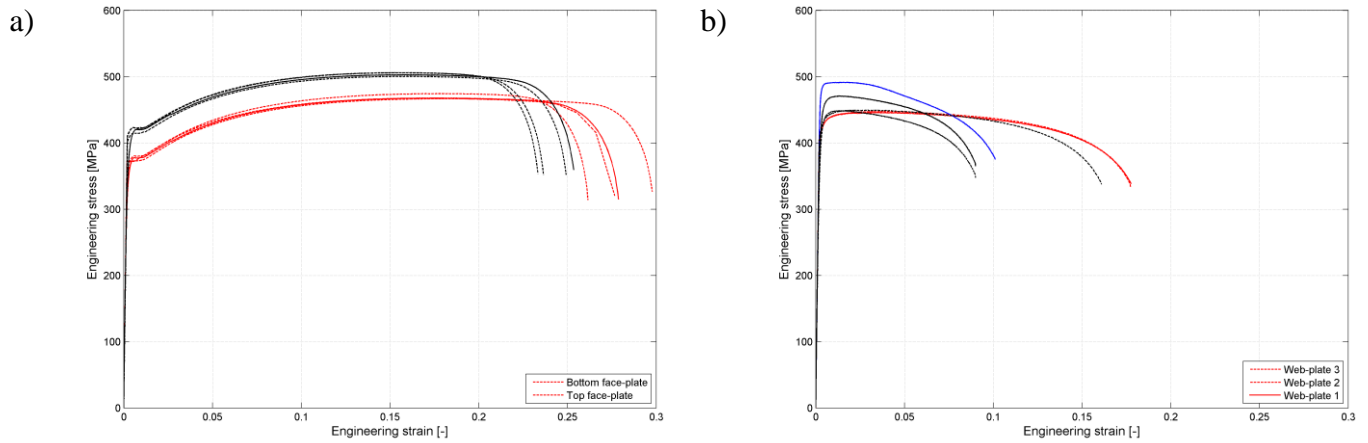


Fig. B.1. Actual and average engineering stress-strain curves for a) face-plates; b) web-plates of the uncorroded beam.

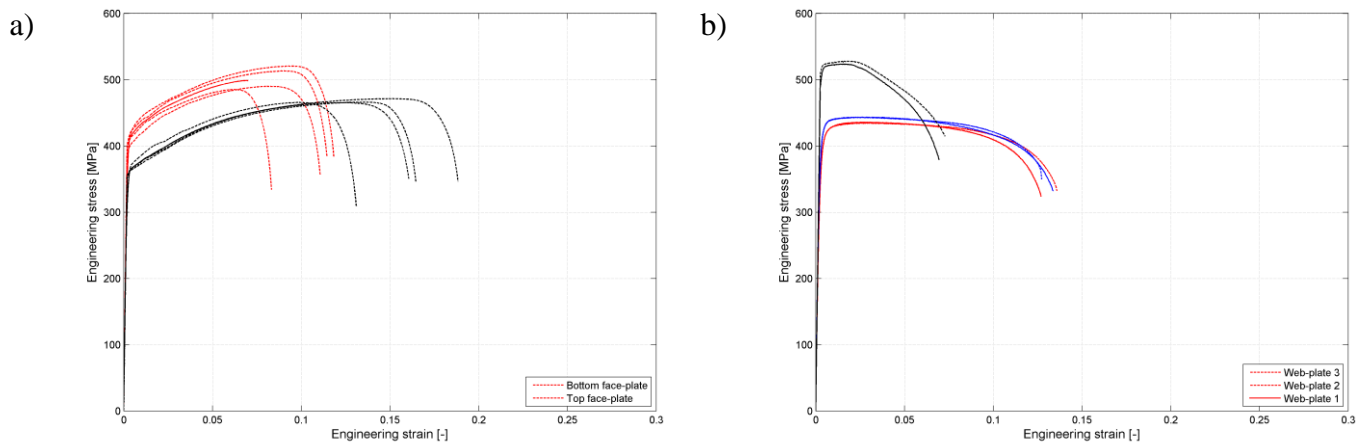


Fig. B.2. Actual and average engineering stress-strain curves for a) face-plates; b) web-plates of the one-year corroded beam.

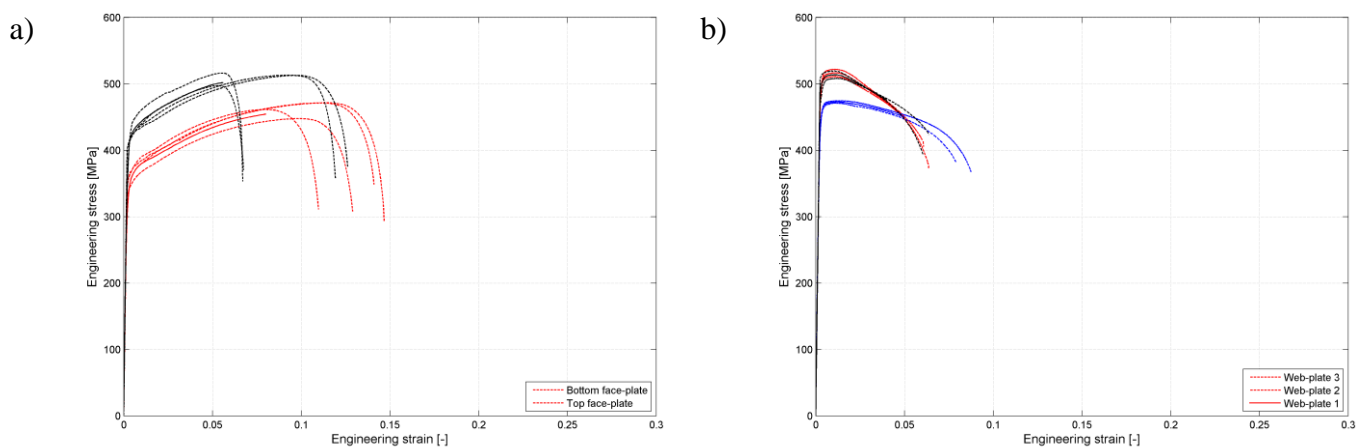


Fig. B.3. Actual and average engineering stress-strain curves for a) face-plates; b) web-plates of the two-year corroded beam.

7 Acknowledgments

This work was supported by the Graduate School of Engineering Mechanics, funded by the Finnish Academy of Sciences, and the *Closed, Filled Steel Structures* project funded by the 100-year Anniversary Funds of the Association of Finnish Industries. The ultimate strength experiments were performed in the Laboratory of Mechanics of Materials at Aalto University. The specimens were prepared in the Laboratory of Corrosion and Material Chemistry and in the Marine Technology group at Aalto University. This support is gratefully acknowledged.

8 References

- [1] P. Kujala, A. Klanac, Steel sandwich beams in marine applications, *Shipbuilding* 56 (2005) 305-314.
- [2] H. Kolsters, P. Wennhage, Optimisation of laser-welded sandwich panels with multiple design constraints, *Marine Structures* 22 (2009) 154-171.
- [3] H. Kolsters, D. Zenkert, Buckling of laser-welded sandwich beams: ultimate strength and experiments, *J. Engineering for the Maritime Environment* 224 (2009) 29-45.
- [4] J. Romanoff, The effect of filling material to the local ultimate strength of an all steel sandwich beam, *J. Structural Mechanics* 35 (2001) 19-39.
- [5] J. Kozak, Problems of strength modelling of steel sandwich beams under in-plate loads, *Polish Maritime Research* 1 (2006) 9-12.
- [6] SANDWICH Consortium, Synthesis report test results, TNO.ALL.Deliverable4.4-v1 03-03-03, 2003.
- [7] Det Norske Veritas "Seawater exposure of laser-welded sandwich beams for evaluation of corrosion properties", Technical report No. 2003-1553, 2003.
- [8] R.E. Melchers, M. Ahammed, R. Jeffrey, G. Simundic, Statistical characterization of surfaces of corroded plates, *Marine Structures* 23 (2010) 274-287.
- [9] B. Boon, B.C. Buisman, T. Luijendijk, R. Vonk, The influence of corrosion on the strength of ship structures, *Proceedings of Eurocorr '98* (CD Rom), Utrecht, Netherlands, 1998.
- [10] A. A. Almusallam, Effect of degree of corrosion on the strength properties of reinforcing steel bars, *Construction and Building Materials* 15 (2001) pp. 361-368.
- [11] M.M. Ahmmad, Y. Sumi, Strength and deformability of corroded steel plates under quasi-static tensile load, *J. Marine Science and Technology* 15 (2010) 1-15.
- [12] M.R.Islam, Y. Sumi, Geometrical effects on strength and deformability of corroded steel plates, in: C. Guedes Soares, W. Fricke (Eds.) *Advances in Marine Structures*, Taylor & Francis Group, London, 2011, pp. 151-159.
- [13] J. Aromaa, J. Leino, A. Pehkonen, J. Virtanen, Corrosion of steel cell structures in seawater, Aalto University series TT 8/2011, 2011.
- [14] J. Jelovica, J. Romanoff, S. Ehlers, H. Remes, Ultimate strength tests of corroded web-core and corrugated-core sandwich beams, Aalto University series, ISBN 978-952-60-4434-7 (electronic publication), 2011.
- [15] Det Norske Veritas "Rules for Ships / High Speed, Light Craft and Naval Surface Craft", Pt.2. Ch.1. Sec.2, 2003.
- [16] M. Jutila, Failure mechanism of a laser stake welded T-joint, Master of Science thesis, Helsinki University of Technology, 2009.

Jelovica, J., Romanoff, J., Ehlers, S., Aromaa, J. “Ultimate strength of corroded web-core sandwich beams”.
Marine Structures 31 (2013) p.1-14.

- [17] J. Romanoff, H. Remes, G. Socha, M. Jutila, P. Varsta, The stiffness of laser stake welded T-joints in web-core sandwich structures, *Thin-Walled Structures* 45 (2007) 453–462.
- [18] C. Guedes Soares, Y. Garbatov, Reliability of maintained, corrosion protected plates subjected to non-linear corrosion and compressive loads, *Marine Structures* 12 (1999) 425-445.
- [19] J. Guo, G. Wang, L. Ivanov, A.N. Perakis, Time-varying ultimate strength of aging tanker deck plate considering corrosion effect, *Marine Structures* 21(2008) 402-419.
- [20] J. Romanoff, P. Varsta, H. Remes, Laser-welded web-core sandwich plates under patch loading, *Marine Structures* 20 (2007) 25-48.
- [21] F.J. Harewood, P.E.McHugh, Comparison of the implicit and explicit finite element methods using crystal plasticity, *Computational Materials Science* 39 (2007) 481-494.
- [22] R.S.H. Richardson, H. Nolle, Surface friction under time-dependent loads, *Wear* 37 (1976) 87-101.